A synergic integration of desalination and solar energy systems in stand-alone microgrids

Marco Astolfi*, Simone Mazzola, Paolo Silva, Ennio Macchi

Politecnico di Milano, via Lambruschini 4, 20156 Milano, Italy

In this study, we investigated the possible synergies between desalination technologies and solar energy in a remote energy system modelled as a small-size island with the goal to increase system sustainability. The solar systems implemented are photovoltaic panels (PV) and a Concentrating Solar Power system coupled with an Organic Rankine Cycle (CSP-ORC). For the desalination both Reverse Osmosis (RO) and Multi-Effect Distillation (MED) are considered. We found that the simple installation of PV is a valuable option to decrease electricity costs in remote context presently based on Diesel fuel generators but it struggles with achieving high penetration of Renewable Energy Sources (RES) (> 40%) due to the intermittent nature of solar energy and the consequent need for large batteries. The installation of a CSP-ORC allows further reducing the fossil fuel consumption thanks to the use of thermal energy storage and the effective integration with a MED facility. The results show that both solar energy technologies allow a considerable cost saving compared with the traditional solutions based on diesel generation. The most promising solution is a hybrid integration of all four above mentioned technologies, enabling RES penetration over 75% with > 10% of cost savings.

Keywords: Island energy access, Hybrid RO/MED, Solar energy, Concentrating solar power, Optimal microgrid management, Renewable sources penetration

1. Introduction

Nowadays most of small islands around the world are still basing their electricity generation on fossil fuels, especially Diesel oil. In fact, in most cases grid connection to the mainland is practically unfeasible or too costly, so that the energy needed to cover the community requirements is produced locally using Diesel oil fueled internal combustion engines with several drawbacks. Since Diesel oil supply has generally a high cost in remote locations (0.8–1.2 USD/l) and diesel generators are often forced to part-load operation throughout the year, the resulting levelized cost of electricity (LCOE) is on average considerably higher (0.3–0.6 USD/kWh) than the one on the mainland [1]. Other relevant shortcomings are related to the strong dependency from an external source, with price fluctuations and uncertainty of supply, and of course the environmental concerns associated to diesel engines emissions.

Problems related to Diesel oil exploitation for electricity generation are even more significant in case of scarcity of fresh water, a situation that may occur in many islands. Since the import is frequently an expensive option, fresh water is usually produced locally from seawater using desalination processes which require considerable amount of electricity [2]. As a consequence, a relevant share of electricity is spent in water desalination, like in the case of Canary Islands where depending on the season from 5 to 30% of electricity is used to power reverse osmosis (RO) plants [3]. The sum of all these factors leads to high expense for fossil fuel import, which in island communities accounts for a value typically ranging from 8 to 20% of GDP, a high value compared to the average one on mainland (4.5%) [4,5].

A possible option to be considered is the installation of power generators based on Renewable Energy Sources (RES). Thanks to the massive deployment of certain technologies (photovoltaic above all), in the last decades a considerable cost reduction has been observed making these technologies competitive with conventional fossil fuels generation. The competitiveness and the advantages are more evident in remote locations, where the cost associated to energy production from Diesel oil is high.

A lot of research and demonstration projects have been conducted to bring RES in islands, with several successful examples [6]. Real cases show that the introduction of solar photovoltaic (PV) or wind turbines (WT) into existing grids historically based on Diesel engines allows considerable fuel and money savings during the project lifetime [7]. However, the most implemented technologies (PV and WT) are based on intermittent sources. Discontinuous and random production poses severe technical issues that are even more challenging to be managed in limited capacity grids. El Hierro, which claims to become the first 100% renewable island, exploiting its wind resource, has experienced several

Received 7 October 2016;
Received in revised form 21 March 2017;
Accepted 17 May 2017
Available online 27 June 2017

* Corresponding author.
E-mail address: marco.astolfi@polimi.it (M. Astolfi).

Published Journal Article available at http://dx.doi.org/10.1016/j.desal.2017.05.025

problems to exceed 30% penetration of RES. The objective will be reached thanks to a hydro-pumped storage system exploiting the peculiar topography of the island [8]. The trend is confirmed in many islands and it is very rare that more than half of energy is produced by RES, even in presence of energy storage systems [7].

One possibility of increasing the dispatchability of RES has been studied by exploiting the potential synergy with desalination. Powering the desalination plant with energy coming from RES in island context leads to both peak shaving and fresh water production cost reduction [1,9]. In this paper we focus on solar energy as RES comparing the advantages attainable with the introduction of two different solar power plants, namely PV and Concentrating Solar Power (CSP) plant. Despite of high installation costs, CSP technology is expected to reach higher RES penetration thanks to the possibility of efficiently storing thermal energy, thus decoupling the electricity production from solar energy availability. Another potential advantage is related to possible synergies with Multi Effect Distillation (MED) plants; this technology, used to produce fresh water, requires huge amount of low-temperature thermal power during operation which could be efficiently produced by the CSP in cogenerative configuration. This option, already investigated for other kinds of Combined Heat and Power (CHP) plants [10], could lead to a reduction of total fossil fuel consumption, potential cost savings in electricity generation and a better exploitation of the solar resource [11].

With the aim of performing a fair and realistic comparison between the two technologies, the whole hybrid system operation is simulated using a rolling horizon approach based on the Unit Commitment problem. Operational costs are assessed simulating a whole year by means of an optimization model which exploits a given set of units, both power generators and desalination plants, to cover the electricity and fresh water demand at the least feasible costs [12]. This is an important novelty compared to other recent studies [10,11,13], in which the performances of the system are evaluated only at nominal or average load and do not take into account the yearly variability of water and electricity demand, the RES productivity and the presence of electric or thermal storage systems.

2. Test-case description

The test-case used to assess the different microgrid (MG) configurations consists of a small island community. The MG is responsible to satisfy both electricity and potable water needs. Due to the lack of comprehensive studies and data availability about one single real case, we built synthetic time series of the demand of both electricity and potable water considering both realistic weather data and a seasonal variability of the island inhabitants. We assumed the weather data of Tenerife (Canary Islands) and used as reference SWEC[1] hourly dataset. In addition, we assumed that island occupancy ranges from 8400 in low season (October–May) up to a peak of 12,000 inhabitants in high season (August).

We split electricity demand per capita in two different terms: basic needs (BN) and air conditioning needs (ACN). The basic needs comprise the domestic and the commercial users, the public lighting and the public buildings loads. We assumed a daily pattern common to most of developed countries, with two demand peaks at the middle and at the end of the working day and a lower consumption during nocturnal hours [14] as reported in both Fig 1.b and c. The daily base electrical load profile is obtained imposing an average electricity consumption of 5 kWh_{el}/(day person) as representative of a developed country. Fig. 1.a depicts the hourly electrical load and the average monthly load along one representative year. The hourly demand peak is in summer and it is about 7 MW_{el} because of the increase of island inhabitants as well as of

[1] SWEC (Spanish Weather for Energy Calculations) data set from https://energyplus.net/weather.

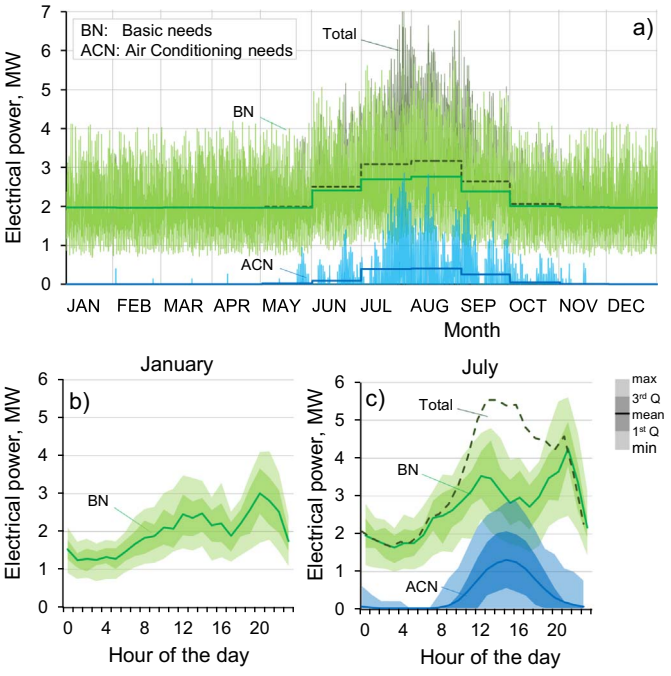

Fig. 1. Trend of electricity consumption: a) hourly variability for the basics needs (light green) and the air cooling load (light blue) and monthly average values. Hourly variability range for the months of January (b) and July (c). (For interpretation of the references to color in this figure legend, the reader is referred to the web version of this article.)

the presence of air conditioning load. In order to simulate the variability of electricity demand, a ± 40% random deviation is added for the basic needs trend while the air conditioning load variation is exclusively due to ambient temperature change. Air conditioning need (ACN) increases proportionally with the ambient temperature when it is higher than 26 °C while vanishes at lower temperatures and its maximum value is assumed equal to the 50% of the BN yearly peak. As result, ACN represents the 12% of electrical energy needs in summer months and 5% on a yearly base. Fig. 1.b and c depict the data variability for January and July reporting for each hour of the day the monthly minimum, the average and the maximum values together with the 1st and the 3rd quartile values of the distribution. The resulting total annual electricity demand (not including water related requests) is about 16.9 GWh.

The daily potable water consumption pattern per capita has been derived from [15] considering that most of the consumption is related to residential and commercial sector (restaurants and hotels). We assumed a daily average consumption equal to 500 l/(day person), with a small seasonality related to ambient temperature. A random variation of ± 10% is added in order to examine a more realistic case. The

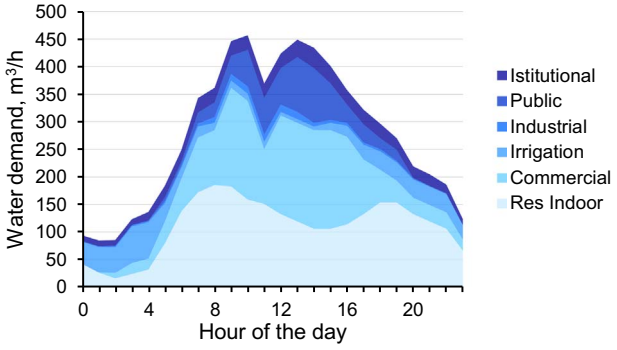

Fig. 2. Daily pattern of community water consumption in the 15th of August.

Table 1
monthly weather data and microgrid goods demand.

Month		Jan	Feb	Mar	Apr	May	Jun	Jul	Aug	Sep	Oct	Nov	Dec	Year average
Ambient temperature	°C	17.9	18.1	18.6	19.2	20.5	22.3	24.6	25.0	24.3	22.4	20.7	18.7	21.0
GHI	kWh/m^{2}day	4.93	5.76	6.15	6.14	6.81	6.72	7.17	7.35	6.58	6.06	5.41	4.82	6.16
DNI	kWh/m^{2}day	3.69	4.52	5.56	6.17	6.89	7.12	7.27	6.95	6.05	4.92	3.94	3.43	5.55
Inhabitants	–	8400	8400	8400	8400	8400	10200	11400	12000	10200	8400	8400	8400	9256
Water (average)	m^3/day	3424	3424	3995	3995	4565	5543	6196	6522	5543	4280	3424	3424	4536
Water (Peak)	m^3/h	240	243	276	284	320	388	434	457	388	300	242	241	–
Electricity	MWh/day	40.2	40.0	40.2	40.0	41	52.7	71	75.4	60.1	43.5	40.5	40.0	48.7
BN	MWh/day	40.2	40.0	40.2	40.0	40.4	50.6	62.1	65.2	54.0	42.1	40.3	40.0	46.3
ACN	MWh/day	0.0	0.0	0.0	0.0	0.6	2.1	8.9	10.2	6.1	1.4	0.2	0.0	2.5
Peak	MW	4.12	4.04	4.00	4.19	4.16	5.16	7.08	6.77	5.84	4.16	4.02	4.16	–

resulting total annual water request is about 1.600.000 m^3 and the aggregate community water need pattern for the 15th of August is reported in Fig. 2.

Table 1 summarizes the monthly data for the test-case in terms of weather information, and microgrid requests.

3. Microgrid configurations and main components description

The simplest plant layout able to satisfy both community needs (i.e. electricity and potable water) is made by a fossil fuel generator and a desalination plant. In the specific case, the MG base configuration (MG0) is provided with three diesel Internal Combustion Engines (ICE) of the same size and a Reverse Osmosis plant (RO). The RO plant is designed to cover the maximum daily demand along the year while the ICEs must cover the MG peak load working together at nominal load. The choice to adopt multiple ICEs in parallel is motivated by the large load variation along the year and with the aim of reducing the annual fuel consumption by limiting part load operation. This assumption also reflects the common practice adopted in islands where a multiple engine configuration is preferred for availability purposes.

In the RO plant, seawater is pumped from the sea and it firstly flows through a series of filters and water treatment units in order to remove the suspended materials and to limit biofouling [3]. After that, it flows in a pressure exchanger device where the pressure is increased at the expenses of the high pressure brine released from the membrane retentate side.[2] The high pressure sea water then enters a set of osmosis membranes working in parallel where pure water is separated and eventually stored in a pool or a tank. Generally, a second stage at a lower pressure is used to maximize the system productivity. The RO specific electric consumption ranges between 3.5 and 5 kWh$_{el}$/m^3 [16] depending on many factors like sea water salinity, components efficiency, membrane configuration and retentate-feed ratio. In the future RO consumption is expected to touch 2.5 kWh$_{el}$/m^3 [3,17], but in this work a value of 4.2 kWh$_{el}$/m^3 is considered as representative of the current average scenario. The MG described is the most common configuration for production of both electricity and potable water [3] but it totally relies on fossil fuel availability with issues in terms of sustainability and operational costs.

In this work other four different microgrid configurations are studied with the aim of increasing system sustainability and of reducing fuel consumption. In the first configuration (MG1) a Multi Effect Distillation (MED) is added to the base case. Photovoltaic panels (PV) and Concentrating Solar Power technology coupled with an Organic Rankine Cycle (CSP-ORC) are investigated in the second (MG2) and in the third case (MG3) respectively while the fourth case (MG4) is focused on the combination of both renewable energy systems. Fig. 3 depicts the most comprehensive MG studied in this work.

[2] In recent years, pressure exchangers are the most common solutions and have replaced turbopumps because of the higher system efficiency [3].

The first possible improvement respect to MG0 considered in this work is to exploit the available heat recoverable from the ICEs[3] to produce potable water with a MED system (MG1). This technology consists in a series of chambers at different pressures where pure water is evaporated from the brine. The highest temperature chamber uses the heat provided by an external source while in the other chambers the heat is provided by the condensation of the steam produced in the previous one. To produce one cubic meter of desalinated water the MED technology requires about 60 kWh$_{th}$ (usually in the range 55–70 °C) and 1.5 kWh$_{el}$ [18,19], thus allowing for a considerable reduction of the electrical consumptions compared to RO technology. Considering reasonable values for a MW-scale diesel CHP engine we assume nominal electrical and thermal efficiencies respectively equal to 43.7% and 35.9%. Assuming to use the electricity only for water production and to operate the system at nominal point, we calculated that an integrated ICE + (RO & MED) system allows to produce more potable water (+ 3.70%) than an ICE + RO system starting from the same fossil fuel amount, thanks to the possibility of exploiting the waste heat with environmental and potential economic benefits.

In the second case (MG2), PV panels are added to the microgrid. Electricity is produced by conventional polycrystalline silicon cell modules in DC and it is converted in AC with an inverter. This solution aims at reducing the fuel consumption mainly in the central hours of the day but it requires an electrochemical storage system (ESS) made by a set of lithium-ion batteries to limit energy dumps and increase the dispatchability of the produced energy.

In the third case (MG3), instead, solar energy is collected by a Solar Field (SF) made by arrays of SkyFuel-SkyTrough collectors loops with 2008 Schott PTR70 Vacuum receiver. Dowtherm A is used as Heat Transfer Fluid (HTF) because of its low freezing point temperature and it is heated up in the SF from a temperature of 180 °C up to 300 °C. The solar field area is calculated starting from the thermal power required by the ORC at full load, by assuming a Direct Normal Irradiation (DNI) equal to 800 W/m^2 and by considering a Solar Multiple[4] (SM). The thermal energy can directly feed an Organic Rankine Cycle (ORC) or it can be stored in a Thermal Energy Storage (TES). The TES system is designed as a single tank thermocline filled with quartzite sand with the goal of reducing the total mass of HTF.

ORC is a well-established technology that is able to efficiently exploit medium/low temperature heat sources of limited capacity. Compared to geothermal and biomass technologies, CSP applications are still limited [20] because this technology shows a nominal sun-to-electric efficiency comparable to PV but it requires a more complex and costly system. However, CSP can use a high efficiency storage thus

[3] Low temperature heat is available from the cooling of (i) the flue gases, (ii) the engine cooling water and lubricating oil circuits, (iii) the Exhaust Gas Recirculation loop and (iv) the Charge Air Cooler.

[4] Solar multiple is the ratio between the actual solar field area and the solar field area required to operate the power block at full load with nominal DNI. It is always greater than one.

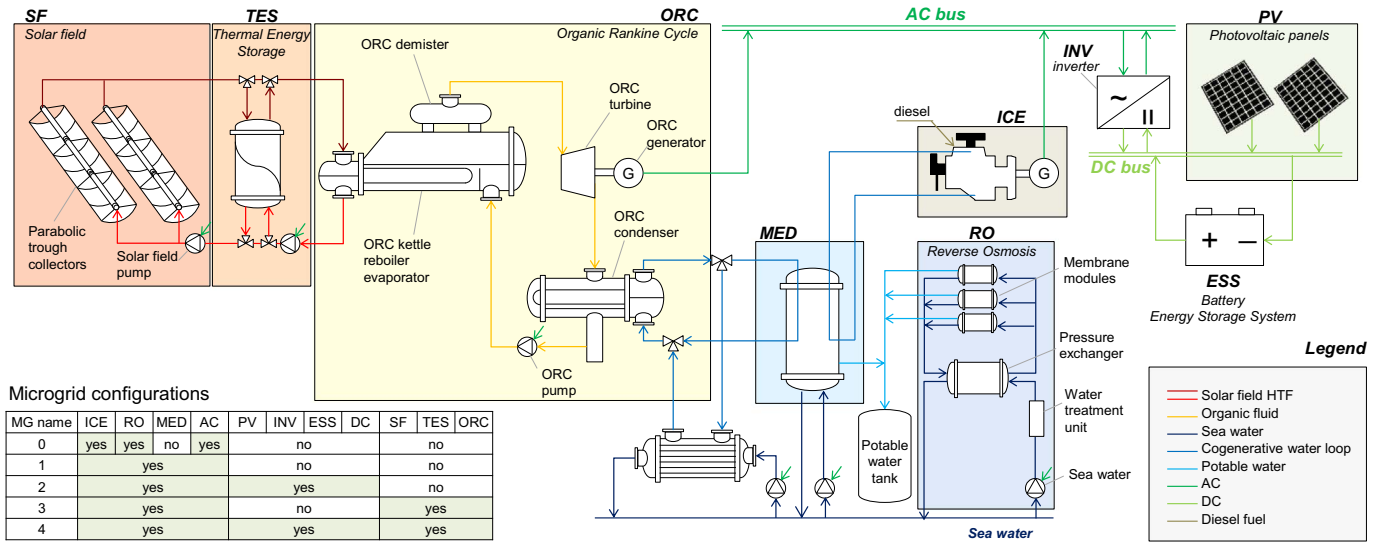

MG name	ICE	RO	MED	AC	PV	INV	ESS	DC	SF	TES	ORC
0	yes	yes	no	yes	no				no		
1	yes				no				no		
2	yes				yes				no		
3	yes				no				yes		
4	yes				yes				yes		

Fig. 3. Scheme of the most comprehensive microgrid analyzed in the study. In the table on the left corner the list of the components used in each microgrid configurations is reported.

allowing for a higher dispatchability compared to PV. We expect that, in off-grid application, this capability could play a relevant role, leading to higher annual performance and possibly a lower Levelized Cost of Electricity (LCOE). In the present case, the ORC is arranged as a sub-critical saturated cycle working with an organic fluid (e.g. pentane). The cycle is recuperative and the condensation heat is released to a closed loop of water. Water can eventually release the heat to a MED system or to the sea water with the possibility to operate the ORC in both cogenerative and pure electric production mode. The nominal ORC electrical efficiency is computed assuming a second law efficiency equal to 55%[5] for the cogenerative mode that leads to an efficiency value equal to 18.6%. In pure electric production mode, the turbine is expected to have a lower efficiency because of the larger enthalpy drop: a penalization (3 percentage points of the second law efficiency) is accounted and the resulting efficiency is 21%. Fig. 4 depicts the Sankey diagram of the ORC in both cogenerative and pure electric operation with a fixed value of 100 kW heat input from the HTF and using the entire electricity production for water desalination with a RO & MED system. It can be seen that the two solutions yield similar results. In case of a RO specific consumption of 4.2 kWh_{el}/m^3, as assumed in this paper, it is convenient to operate the ORC in cogenerative mode, recovering the available heat with the MED system, while, with a more efficient next generation RO system (2.5 kWh_{el}/m^3) would be more convenient to produce potable water only by reverse osmosis.

Finally, the fourth MG configuration (MG4) considers the integration of both PV and CSP plants for a higher penetration of Renewable Energy Sources (RES). In all the three hybrid diesel/solar MG configurations a combination of RO and MED can be used in order to better exploit the heat available from both the diesel engines and the ORC in cogenerative operation. The optimal ratio between MED and RO nominal capacities changes depending on the efficiency of RO system and the size of the ORC. Fig. 5 reports the interconnection between the different components and the goods handled by the MG namely (i) the DC electricity stored in the ESS, (ii) the AC electricity, (iii) the high temperature heat stored in the TES, (iv) the low temperature heat and (v) the potable water that can be stored in a pool. Regarding the above mentioned goods, only DC electricity, high temperature heat in the TES and water are considered storable. Among these ones the high tem-

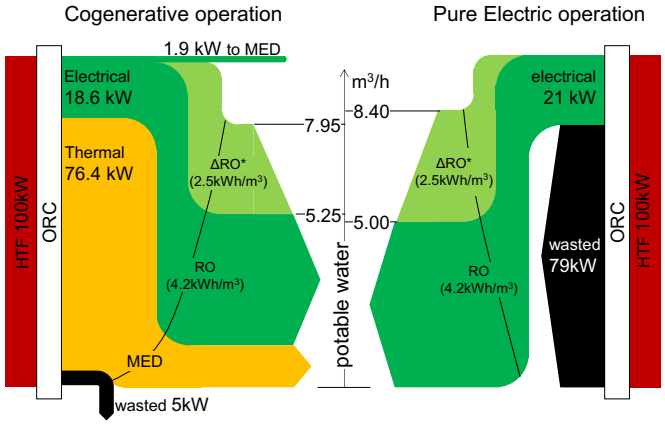

Fig. 4. Sankey diagrams for potable water production for the ORC working in cogenerative mode (on the left) and in pure electric production mode (on the right). Light green represents the additional potable water that would be produced with a more efficient RO system. (For interpretation of the references to color in this figure legend, the reader is referred to the web version of this article.)

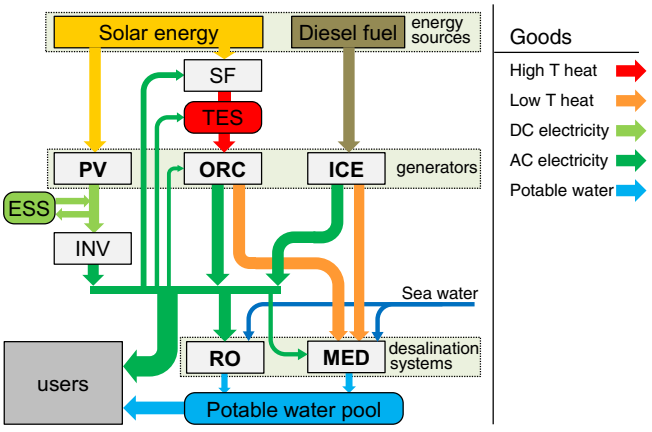

Fig. 5. Scheme of the interconnection between the microgrid components and goods.

[5] Second law efficiency is computed with respect to the reversible Lorenz cycle working between the HTF mean logarithmic temperature and the condensation temperature equal to 65 °C and 30 °C for the cogenerative and the pure electric operation mode respectively.

Table 2
Nominal and off-design performance of the microgrid components and their minimum load constraints.

			Nominal performance		Part load[a]			Min load	Startup costs[b]
			Index	Value	A	B	C	Value	Value
Generation	ICE		η_{el}	43.70%	− 0.17	0.32	0.31	25%	8%
			η_{th}	35.90%	0.17	− 0.32	0.51		
	ORC	Pure electric T cond = 30 °C	η_{el}	21%	− 0.05	0.1	0.16	30%	30%
		Cogenerative T cond = 65 °C	η_{el}	18.60%	− 0.05	0.09	0.14		
			η_{th}	76%	0.05	− 0.091	0.81		
Desalination	RO		kWh_{el}/m^3	4.2				20%	5%
	MED		kWh_{el}/m^3	1.5				40%	30%
			kWh_{th}/m^3	60					
Others	Lithium battery		$\eta_{round\ trip}$	91%	− 0.05	0.02	0.95		
	Bidirectional inverter		η_{AC-DC}	90%					
			η_{DC-AC}	94%					

[a] Part load efficiency is defined with a parabolic function in the form $\eta = Ax^2 + Bx + C$ where x is the percentage of maximum power.
[b] Relative startup costs refer to the hourly consumption at nominal load.

perature heat is the only good which has a loss factor[6]: each hour, 2% of energy stored is lost to environment. Table 2 reports the assumed efficiencies of the different MG components considered in this study.

4. Optimal microgrid management and design

In this section, we give an overview of the methodology used to assess the techno-economic performance of different MG configurations. Fig. 6 depicts the outline of the proposed method.

The optimal MG design is found by investigating different combinations of components size. Except for the ICEs whose sizes are fixed, the most complicated MG, among those studied, requires the definition of 7 parameters[7]: the nominal power of both (i) the PV and (ii) the ORC plants, (iii) the Solar Multiple of the solar field, the capacity of both (iv) the battery and the (v) TES and the nominal productivity of both (vi) the RO and (vii) the MED systems. Water storage capacity is another variable, but we decided to fix it to 13,000 m^3 (equivalent to 2-days water request in the most demanding month), since it is expected to have a low cost compared to other components and the simulations do not show any advantage in a further capacity increase. Many different combinations of components size must be analyzed with the aim of minimizing the MG total annualized cost. The combinations can be selected mainly with two strategies [21]: the first requires a proper optimization algorithm (like a Genetic Algorithm) while in the second a fixed number of combinations is explored with an enumerative approach. The first method suffers from the presence of local minimum while the second may be penalized by a long computational time if a very dense discretization of the components size is adopted. In the present study the latter approach is implemented in order to obtain a clearer representation of the influence of the different variables and avoid local minimum.

Table 3 reports the components whose size must be optimized for each MG configuration and the range of components size investigated. A preselection of the combinations is required in order to exclude those designs that are not reasonable like large PV plants without battery or a total desalinated water capacity largely above the maximum daily request.

For each case the hourly productivity of PV and CSP plants have been evaluated using SAM [22] considering reliable weather data and

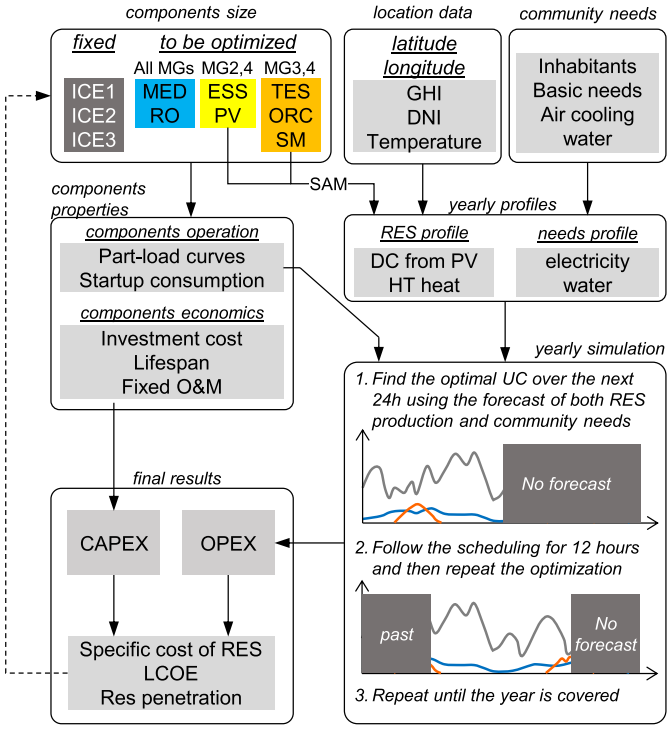

Fig. 6. Flowchart of the assessment method for MG configurations performance.

referenced components efficiency while the electricity and the potable water requests are equal for all the cases and rely on the assumptions reported in Section 2.

For each case, the total annualized cost is then computed optimizing the MG operation over one year namely defining the optimal schedule of all the dispatchable generators and schedulable loads. This goal would be accomplished by solving a single one-year Unit Commitment (UC) problem with the aim at minimizing the cost of operation. This approach is extremely time consuming because of the size of the optimization problem (8760 h) and a Rolling Horizon strategy with multiple unit commitment calls is strongly suggested in these cases [21]. The steps involved in this method are the following:

1. At time step *t*, the forecast of goods demand and the RES production for the next 24 h is evaluated
2. Knowing the forecast and the units operational constraints, the

[6] Battery energy losses are taken into account with charge and discharge efficiencies.
[7] The number of parameters to be optimized is lower for the other microgrid configurations. In particular it is necessary to optimize two parameters in the first case, four in the second case and five in the third. The base case (MG0) is not optimized since the size of diesel fuel engines and RO system are selected to satisfy the peak load of electricity and water.

Table 3
Minimum and maximum size of the MG components subject to optimization and step used for the discretization for each different MG configuration.

	Unit		Min	Step	Max	Case			
						MG1 ICE + (RO & MED)	MG2 (ICE & PV) + (RO & MED)	MG3 (ICE & CSP) + (RO & MED)	MG4 (ICE & PV & CSP) + (RO & MED)
Generation	PV	MW	0	1	16		X		X
	ORC	MW	0	1	5			X	X
Solar field	Solar multiple		1	0.5	3			X	X
Storage	Battery	MWh	0	0.5	32		X		X
	TES	hours	6	2	12			X	X
Desalination	RO	m^3/day	0	500	8000	X	X	X	X
	MED	m^3/day	0	500	8000	X	X	X	X

optimal schedule of the available units is obtained solving the UC for the next 24 h
3. The schedule is followed for 12 h
4. The value of t is updated at $t = t + 12$ and the process is repeated

Each single unit commitment problem aims to find the most cost-effective schedule of the available generators to cover the demand over a certain time span, called time horizon (24 h in the present study). The objective function to be solved is the following:

$$min\, C_{opex} = \sum_{t\in T} \left(\sum_{i\in U} \left[c_{t,i}^{var} + c_{t,i}^{startup}\right]\right) \quad (1)$$

where $c_{t,i}^{var}$ is the cost of operation for the generic unit i and it comprises the variable O & M cost plus the fuel cost for the ICE and the wear cost for the battery. As already stated in the Introduction, diesel oil can have a very high cost in remote locations, because of the transportation costs: for this reason, diesel oil price is assumed equal to 1 USD/l, which is a common value in these contexts [23]. For the battery instead, the wear cost takes into account the actual use of the electrochemical storage on the basis of a referenced aging model [24].

The problem, expressed with a Mixed Integer Linear Programming (MILP) formulation, is solved considering a set of operational constraints that represent the technical limits of the components, the spinning reserve requirements and efficiency curves at part load operation. The presence of multiple goods that must be handled contextually by the UC formulation makes the problem more complex but it allows to take advantage of synergies between different valuable assets in the system, ensuring potential cost savings compared with standardized approaches like heuristic strategies. Further details on the problem formulation can be found in [12].

Once the entire year is simulated the total annualized cost of the system (C_{tot}) is calculated summing all the monetary costs associated to units operation (C_{opex}^{year}), the fixed O & M ($C_{O\ \&\ Mfix}$) and the capital costs (C_{capex})

$$C_{tot} = \sum_{i\in U} C_{tot,i} = \sum_{i\in U} \left(C_{opex,i}^{year} + C_{O\ \&\ Mfix,i} + C_{capex,i}\right) \quad (2)$$

The capital cost of the generic component i is defined using the following equation:

$$C_{capex,i} = C_{ref,i}^{*}\left(\frac{size_i}{size_{ref,i}}\right)^{k} CRF_i \quad (3)$$

where $C_{ref,i}$ is the up-front investment cost related to the reference size ($size_{ref,i}$), k is a parameter which takes into account economies of scale and CRF_i is the capital recovery factor of unit i, which is a function of the interest rate (assumed equal to 9%) and the lifetime of the component. All the economic assumptions of this study are reported in Table 4. The cost of traditional components (ICEs, PV plant, Li-on battery and bi-directional inverters) are obtained from retailers' public websites while Solar Field costs are derived from SAM default values [25]. The module cost of the ORC is assumed equal to 1400 USD/kW_{el} with an exponential coefficient of 0.8 as representative of a multi megawatts cheap ORC unit [26]. Regards desalination plants, economic data are obtained from [27] and the annual O & M for the RO plant includes the replacing cost of membranes which have an average life span equal to 5 years. The specific cost of the present thermocline system is obtained starting from cost information of both conventional double tank storage [28] and high temperature thermocline [29] and applying appropriate scaling factors for the tank material, the fluid and the filling material inventory. The cost of tanks for desalinated potable water has been neglected in this analysis.

5. Results

The results chapter is organized in four sections: in the first the optimization of the components size is carried out in order to find the MG with the lowest total year expenses, in the second the MG levelized cost of electricity is presented as function of the RES penetration, in the third the specific cost for the desalination process is discussed, finally a sensitivity analysis on the capital cost of RO and MED system is proposed.

Table 4
Economic assumptions for the components considered in the MG configurations.

		Up-front costs		annual O & M	Lifetime, years	k, reference size
Generation	ICE	500	USD/kW	10%	10	–
	PV	1300	USD/kW	2%	25	–
	ORC	1400	USD/kW	4%	25	0.8, 1 MW
Storage	Li-ion battery	550	USD/kWh	2%	–	–
	TES	43	USD/kWh_{th}	1%	25	0.8, 150 MWh_{th}
Desalination	RO	800	USD/(m^3/day)	7%	20	–
	MED	950	USD/(m^3/day)	4%	20	–
	Solar field	260	USD/m^2	4%	25	0.9, 45,000 m^2
	Inverter	400	USD/kW	2%	15	–

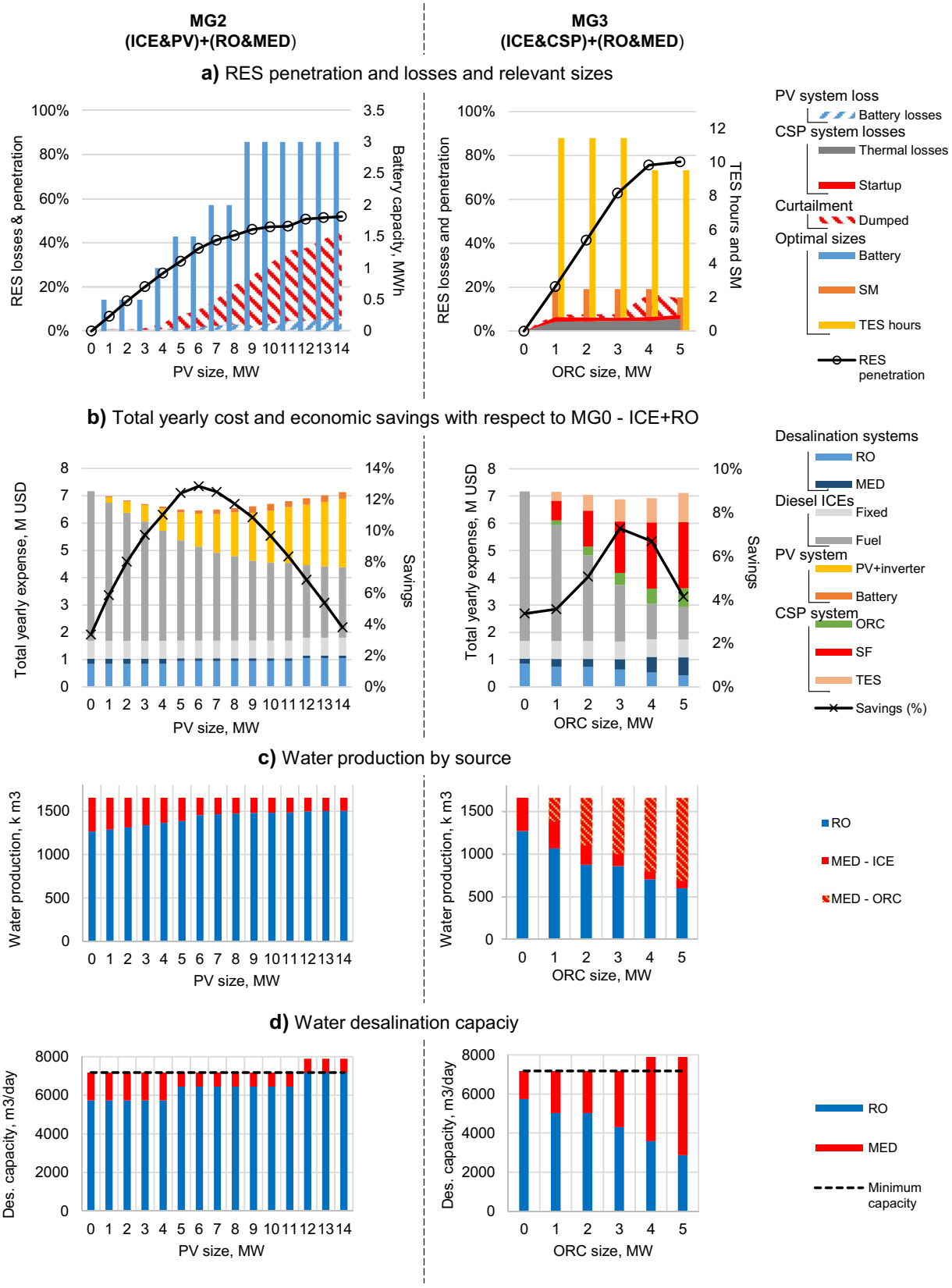

Fig. 7. Trends of relevant figures of merit changing the size of the RES generation technology.

5.1. Optimization of microgrid configuration

The optimal design of the different MG configurations is obtained with the approach described above and investigating several hundreds of combinations according to the size ranges in Table 3. The influence of size of the two renewable components is shown in Fig. 7: figures on the left column refers to the MG2 configuration (ICE & PV) + (RO & MED) and are focused on the PV plant size sensitivity analysis, figures on the right column instead refers to the MG3 (ICE & CSP) + (RO & MED) and depicts the effects of different ORC power outputs.

Fig. 7.a and b illustrate the influence of the renewable plant size on the RES penetration and on the total yearly expenses respectively. Installing a PV plant has the main advantage of reducing the diesel consumption leading to economic benefits but on the other hand it involves the use of a battery. For large PV sizes, the increment of battery capacity required to properly handle the solar production would strongly penalize the MG economics. As result, the optimization algorithm prefers to dump energy in the central hours of the day instead to adopt a big battery bank that would be overdesigned for most of the year. For PV size above 6 MW a large amount of solar energy is wasted with a consequent limitation of RES penetration and electricity production that still largely relies on diesel engines. We find that the optimal solution for PV is an installed capacity of 6 MW (corresponding to 34,600 m^2 of PV panels and 28.8 acres of footprint) with a battery of 1.5 MWh and a RES penetration close to 40%. A further increase of PV size reduces the savings with respect to the reference MG0 - ICE + RO case because of the limited number of equivalent hours of the PV and almost constant fossil fuel consumption.

Similar considerations can be highlighted for the CSP case: the larger is the ORC the higher is the RES penetration and the lower the fossil fuel consumption. Differently from the PV case, the cheaper and more efficient storage system (TES) guarantees a high dispatchability of the solar energy and it allows pushing the RES penetration up to values close to 80%. The optimal size of the ORC is 3 MW with 2.5 SM and 11 h of TES (corresponding to 67,500 m^2 of solar field aperture area, 45 acres of footprint and around 140 kg/s of HTF). Maximum savings in this case are lower than for the PV because of the higher specific cost (USD/kW) of the CSP but this configuration is certainly attractive with the goal of increasing the RES penetration.

Fig. 7.c depicts the optimal size of both the MED and the RO systems increasing the PV and the ORC size while Fig. 7.d shows the contribution to water desalination of the two technologies. When all electricity production is obtained by only Diesel engines the most convenient configuration is represented by a MED system that matches the thermal power released by a single ICE and a RO system able to cover the remaining water demand. ICE runs always in cogeneration (unless the water tank is full) and about 20% of potable is produced by MED. Increasing the size of PV, the contribution of MED decreases, following the decrease of available heat from Diesel. However, the MED capacity remains the same until the reduction of the diesel running hours makes a smaller and cheaper MED more attractive.

On the other hand, when a CSP system is added, the MED can be also fed by the condensation heat of the ORC. Increasing the size of the ORC leads to a large size of the MED system, a large share of potable water produced by MED and a reduction of both RO capacity and production.

According to the results obtained, PV and CSP have a different impact on MG operation. For a better understanding of the capabilities of the optimization algorithm in handling different kinds of MG assets, the operation of four different MG configurations are reported in Fig. 8.a–d for two typical days (representative of winter and summer conditions respectively). The first three configurations refer to the cases already described:a) MG1 ICE + (RO & MED), b) MG2 (ICE & PV) + (RO & MED), c) MG3 (ICE & CSP) + (RO & MED) while the last configuration d) MG4 (ICE & PV & CSP) + (RO & MED) is introduced to highlight the synergies achievable using both solar energy plants. For each configuration, we refer to the optimum combination of design parameters.

The upper part of each figure depicts the diagram of the hourly electrical energy generated by the various components and the charge status of the electrochemical and thermal storages, while the lower part depicts how the electricity is used. In the first configuration battery is not used and the optimization algorithm only defines the RO schedule in order to increase the average load and the efficiency of the diesel engines in operation. Potable water production, and hence RO consumption, is modulated during the day and it is usually higher when the electrical consumption (BN + ACN) is low or when the two diesel engines are running together.

For the second configuration (ICE & PV) + (RO & MED), a battery is indispensable to minimize energy dump. It can be seen that in winter, the energy generated by PV is mainly used in the daily hours: most of the power flows across the inverter while only a small fraction is stored to be used during evening hours. RO is scheduled in the central hours of the day in order to limit the power fluxes through the battery and the associated loss. One diesel engine operates continuously, while a second one is required only for 1 h in the evening. In summer, the PV contribution is larger and a small amount of energy is dumped due to the limited size of both electrochemical storage and RO. The diesel engine contribution is still large and the algorithm keeps one ICE in operation for most of the day in order to limit the startup cost.

For the third configuration (ICE & CSP) + (RO & MED) the solar contribution in winter is limited because of the optical losses that strongly affect linear concentrating collectors. Most of the heat collected feeds directly the ORC, which works in cogenerative mode, while a small fraction is stored in TES to extend the ORC operation in evening hours. Diesel engines still play a relevant role. On the contrary, in summer the ORC production is capable to cover the majority of the electricity demand thanks to the higher available solar energy and the higher solar collectors' efficiency. A single ICE runs close to the minimum load during the central hours of the day guaranteeing a proper spinning reserve and during the evening (when the basic needs are higher). During nocturnal hours the engine is switched off and the TES is discharged. As a general observation, PV technology is characterized by large savings (small capital cost) but it shows severe issues in dispatching energy because of an expensive storage leading in the end to a poor RES penetration. On the other hand, the CSP system capital cost is relevant but the high dispatchability of the stored thermal energy gives a great flexibility to the MG management with a consistent reduction of fossil fuel consumption.

In order to mitigate the drawbacks of both PV and CSP plant while combining their strengths a last configuration (ICE & PV & CSP) + (RO & MED) is investigated. Results are reported in Fig. 8.d. In winter time PV directly feeds the load assisted by a diesel engine while thermal energy from solar field is stored in the TES. The ORC starts up when the PV production decreases and allows to temporary switch off the ICE. During summer the MG operation almost totally relies on solar energy: in particular PV power directly flows through the inverter while the TES is filled. ORC is in continuous operation in order to limit start up penalizations: it works in load-following during the night while during the day it reduces it load working in cogeneration feeding the MED system.

Fig. 9.a–c illustrate the share of electricity produced by the solar energy and the diesel engine for the three optimal hybrid MG configurations. PV production is more constant along the year leading to a RES penetration slightly above 40% in the low season and lower values during the summer when the island inhabitants and the electrical load increase. A similar trend is shown for CSP case with a marked drop of RES penetration in winter time because the poor optical efficiency of the Solar Field. Fig. 9.c depicts the benefits attainable with the synergic adoption of both PV and CSP.

The addition of a CSP system to a PV plant allows to almost double the RES penetration, with values of about 60% in December and January and value close to 80% during all the other months.

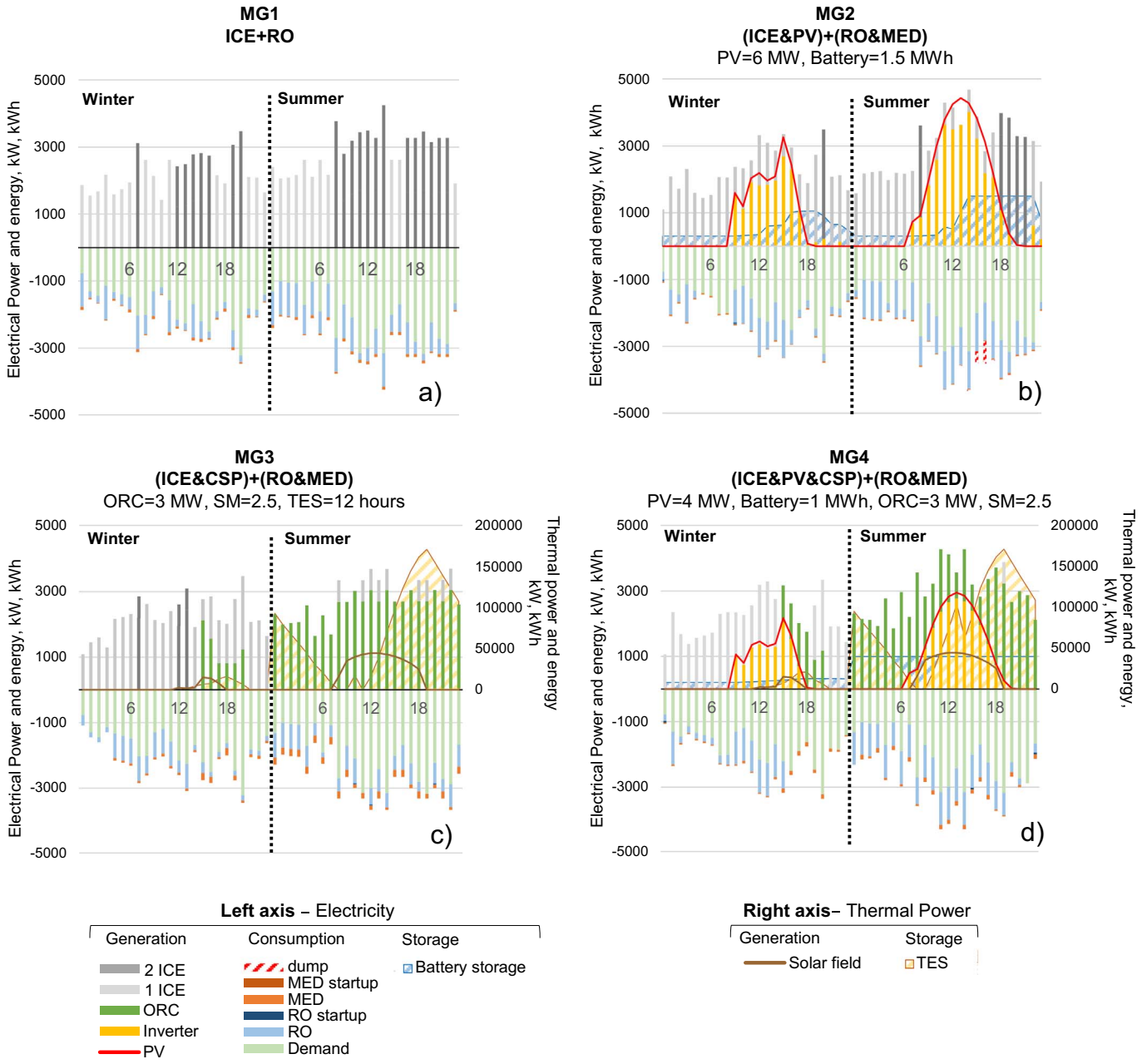

Fig. 8. Two-days optimal schedule for 4 different MG configurations.

5.2. *The effect of RES penetration on MG economics*

Additional hints about RES impact can be found evaluating the specific cost of RES (c_{RES}). The index c_{RES} is representative of the specific annualized cost of the RES power plant and it is equal to the sum of all the expenses (annualized fixed and variable costs) of the RES system divided by the fraction of energy produced which is effectively used to cover the electricity demand. Battery and TES costs are considered as well in the calculation of PV and CSP specific cost respectively. Moreover this index includes the energy losses due to the efficiency of the storage system and the energy dumps due to its limited size.

$$c_{RES} = \frac{C_{fix,RES} + C_{var,RES}}{E_{consumed} - E_{ICE}} \tag{4}$$

Fig. 10.a and b illustrate the specific cost of RES (c_{RES}) for MGs provided by a PV plant and a CSP plant respectively. The configurations shown in this case represent the most cost-effective sizes combination for a given RES penetration (on the x-axis).

PV is the solar technology with the lowest specific cost (around 175 USD/MWh) but it allows achieving a limited RES penetration. In order to reduce the fossil fuel consumption the size of the PV must be increased and this lead to a rapid soar of the battery capacity and a consequent increment of capital and maintenance costs. For small PV sizes the energy produced can be easily handled by a proper schedule of the dispatchable loads or with a small battery, while if the PV rated power is largely above the AC load peak a very big battery is required to accommodate the energy surplus and to increase RES penetration. Battery is used more intensively with a marked wear that impact on the RES specific cost. For RES penetration above 40% we assist to a marked soar of the RES specific cost highlighting that a MG cannot rely only on PV technology and be economically feasible at the same time.

CSP technology instead is more capital intensive, hence its specific cost is higher than PV. However, increasing the size of both the solar field and the ORC allows achieving high RES penetration values with a

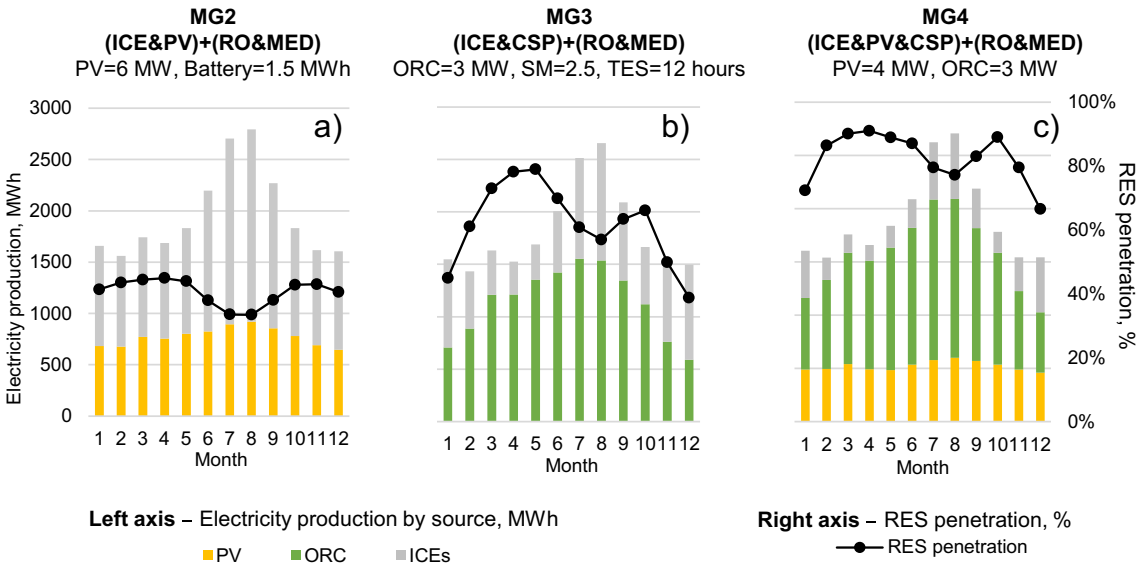

Fig. 9. Monthly trends of electricity production and RES penetration for three MG configurations (ICE + PV, ICE + CSP, ICE + PV + CSP).

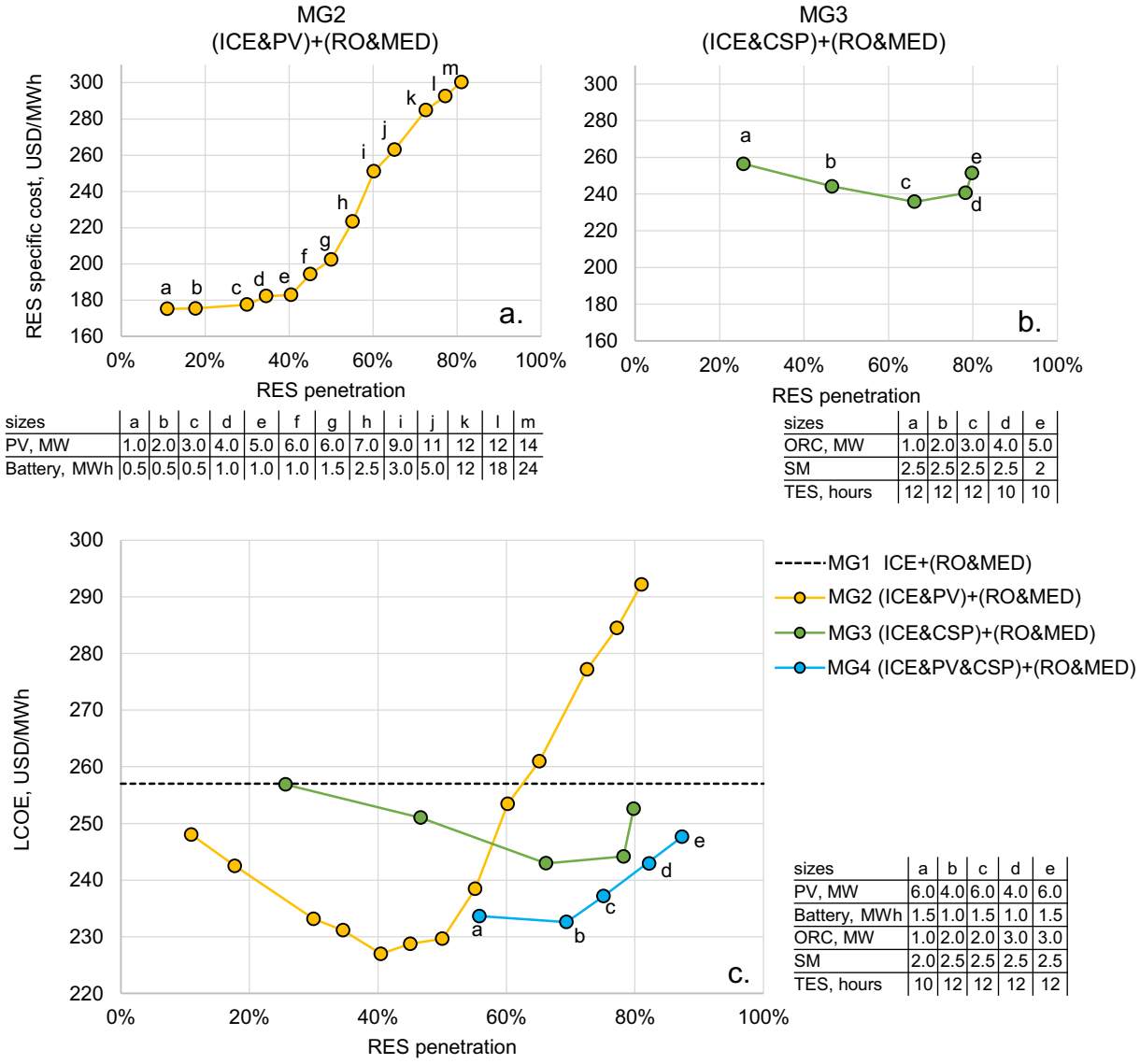

sizes	a	b	c	d	e	f	g	h	i	j	k	l	m
PV, MW	1.0	2.0	3.0	4.0	5.0	6.0	6.0	7.0	9.0	11	12	12	14
Battery, MWh	0.5	0.5	0.5	1.0	1.0	1.0	1.5	2.5	3.0	5.0	12	18	24

sizes	a	b	c	d	e
ORC, MW	1.0	2.0	3.0	4.0	5.0
SM	2.5	2.5	2.5	2.5	2
TES, hours	12	12	12	10	10

sizes	a	b	c	d	e
PV, MW	6.0	4.0	6.0	4.0	6.0
Battery, MWh	1.5	1.0	1.5	1.0	1.5
ORC, MW	1.0	2.0	2.0	3.0	3.0
SM	2.0	2.5	2.5	2.5	2.5
TES, hours	10	12	12	12	12

Fig. 10. RES specific cost and LCOE as a function of RES penetration. The single points represent the optimal sizes for a given RES penetration range.

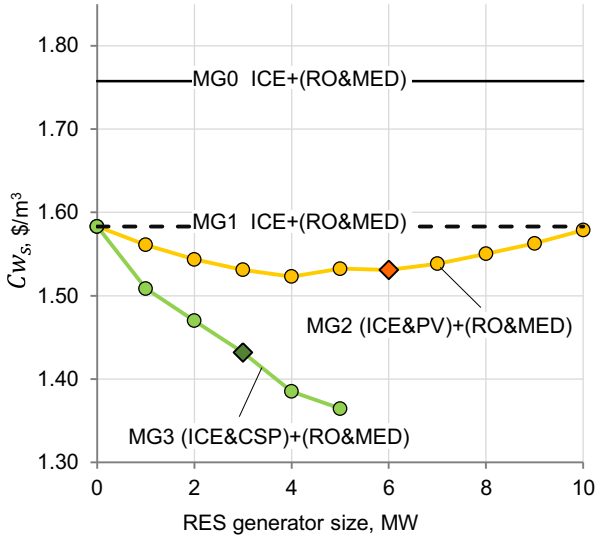

Fig. 11. Specific cost of desalinated water as function of RES generator size. Square marker refers to the MG with the lowest LCOE.

RES specific cost that decreases thanks to the favorable scale economies. In this case it is possible to reach RES penetration close to 80% but a further increase is not possible because of the availability and reliability of the system and the solar mirrors defocusing in the days with high DNI.

Fig. 10.c depicts the LCOE trends in relation to RES penetration for three hybrid MG configurations: the first provided with PV, the second with CSP and the third with a combination of both. The LCOE of the MG provided only by diesel engines plus RO and MED is reported for comparison. LCOE is calculated as the ratio between the total yearly cost (as the sum of the annual operation costs and the annualized investments for all the MG components including the desalination systems) and the electrical energy required by a microgrid provided only by diesel engines and a RO system (base case).

ICE + PV configuration shows the highest savings for a RES penetration around 40–50%, but becomes noncompetitive respect to diesel for RES penetration above 60%. CSP, despite the lower attainable savings, allows to strongly reduce the fossil fuel consumption still remaining competitive up to 80%. Finally, calculations show that with a synergic use of both solar systems it is possible to reach values close to 230 USD/kWh, similar to the ones obtained by the best PV solution, but with a much higher RES penetration (about 70% vs 40%). Moreover it would be possible to break the limit of 80% RES penetration with still relevant economic savings respect to the reference only Diesel case.

5.3. Specific cost of desalinated water

Fig. 11 shows the trend of the specific cost of desalinated water Cw_s measured in $/m^3. This parameter is calculated in an approximate way because, in presence of multi goods units (like the cogenerative ICE and the cogenerative ORC), it is not possible to rigorously divide the fixed and variable costs between the different goods produced. We calculate Cw_s with the following equation where also a fraction of the total annual cost of the power generator units is accounted proportionally to the energy need of the desalination systems respect to the total energy produced by the unit.

$$Cw_s = \frac{\sum_{i\in\binom{RO}{MED}} C_{tot,i} + \sum_{i\in\binom{ICE}{PV}{CSP}} C_{tot,i}\frac{E_{(RO+MED),i}}{E_{prod,i}}}{m^3{}_{water,year}} \quad (5)$$

The introduction of renewable energy sources generators as PV and CSP + ORC systems allow reducing the cost of desalinated water respect to both MG0 and MG1 configurations thanks to the lower cost of electricity and the synergies with cogenerative units. Results are more marked for MG3 (ICE & CSP) + (RO & MED) configuration because thanks to the large amount of potable water produced by the MED plant coupled with the ORC unit. On the contrary, benefits are less pronounced for MG2 and they tend to be null for large PV size because of the relevant energy dump due to the limited size of both the battery and water storage system.

Table 5
Results of the sensitivity analysis on desalination systems capital cost.

Desalination systems specific capital cost				
Scenario	S0	S1	S2	S3
RO USD/(m^3/day)	800	1200	1200	1600
MED USD/(m^3/day)	950	1425	1900	1425
MG1 – ICE + (RO & MED)				
RO/MED	4			
Capex kUSD/year	896.021	1210.21	1254.05	1433.07
Opex kUSD/year	6172.21	6391.94	6407.87	6578.50
Total cost kUSD/year	7169.59	7703.52	7763.29	8112.94
USD/m^3	1.58	1.90	1.941	2.15
MG2 – (ICE & PV) + (RO & MED)				
RO/MED	9			
Capex kUSD/year	2090.52	2393.75	2415.67	2651.31
Opex kUSD/year	4374.55	4603.51	4611.47	4815.87
Total cost kUSD/year	6465.07	6997.26	7027.14	7467.19
USD/m^3	1.53	1.85	1.87	2.13
MG3 – (ICE & CSP) + (RO & MED)				
RO/MED	1.5	1.5	4	1
Capex kUSD/year	3538.85	3874.97	3874.96	4015.62
Opex kUSD/year	3341.23	3542.53	3646.78	3681.50
Total cost kUSD/year	6880.08	7417.49	7521.74	7697.12
USD/m^3	1.43	1.769	1.93	1.85

5.4. Sensitivity analysis on desalination systems capital cost

Finally a sensitivity analysis is carried out in order to evaluate the impact of different capital investment cost of desalination systems on the MGs optimization and economics. We considered three scenarios: in the first (S1) both RO and MED capital costs are increased by 50%, in the second (S2) we increased RO by 50% and MED by 100% while in last case (S3) the opposite. Table 5 reports the results: as general observation, an increase of RO and MED costs directly reflects on both capital and operational costs leading to a more expensive MG and a higher specific cost of desalinated water. More specifically, in MG1 and MG2 configurations we found that the optimal size of generators and the optimal ratio between RO and MED sizes do not change varying the capital cost of desalination systems. In fact, MG1 is provided only by diesel fuel ICE: the low temperature heat recovery does not affect the generator operation and thus it is always profitable to operate the engine in cogenerative mode. Since the diesel engines run most of the year at high load, optimal MED size is large and it almost matches the heat that can be recovered by a single ICE at nominal load. In MG2 instead the availability of PV power leads to a bigger RO size in order to limit the use of the battery while diesel engines run less hours and with a lower average load leading to a smaller MED unit. As a consequence,

RO/MED size ratio for MG1 and MG2 is equal to 4 and 9 respectively. On the contrary in MG3, the non-homogeneous variation of RO and MED costs in S2 and S3 leads to a change of the optimal RO/MED size ratio which is 1.5 in S0 and S1 scenarios. In S2, the higher capital cost of MED involves an increase of RO/MED size ratio up to 4: ORC runs in pure electric generation mode most of the time and MED works mainly coupled with the ICE. On the opposite, in S3 RO/MED size ratio is equal to 1 since the ORC is operated mainly in cogenerative mode and with a high average load in order to take advantage by the less expensive MED system.

6. Conclusions

The present study aims at highlighting the advantages of combining different desalination technologies and different solar power systems in a stand-alone microgrid for both electricity and potable water production. Although the study focuses only on single test case, we expect that the found qualitative trends are representative of a common situation for relatively high insolation islands whereby a significant fraction of the energy demand is devoted to water desalination.

Our conclusions can be summarized in the following points:

- Solar energy plants and desalination units can be integrated in a synergic way provided that their schedule are optimized by an advanced Energy Management System (EMS). The EMS should be able to take into account weather and loads forecast exploiting the possibility of translating the energy required by RO plants in the sunniest hours and limiting the use of the battery. We found that a rolling horizon approach coupled with a 24 h Unit Commitment problem formulated as MILP is an accurate and fast method for this case;
- Both PV and CSP-ORC technologies allow reducing overall cost while increasing the penetration of RES. In particular the PV panels + inverter specific cost have been consistently reduced in the last ten years making this technology extremely attractive until the energy produced can be directly used by the RO plant instead of stored. PV technology is indicated for RES penetration below 40%. Above this threshold the combined effects of larger energy storages and a higher amount of dumped energy lead to a sharp increase of annualized cost. CSP technology allows for smaller savings compared to PV because of the very high investment cost. On the other hand, the use of a TES permits to operate the ORC in a flexible way with the possibility to dispatch energy in an easy and cheap way. This technology benefits from scale economies and working in cogeneration allows for an effective integration with MED system. The highest RES penetration is close to 80%.
- Synergies between all the above mentioned technologies are very promising. The combination of the two solar plant systems, i.e. PV and CSP-ORC, takes advantage from the characteristics of both technologies: the former that generates electricity at a low cost during high insolation hours and the latter that permits to extend the operation in night hours thanks to low cost thermal storage. On the other hand, the combination of the two desalination plant technologies, i.e. reverse osmosis and multi effect distillation, leads to a synergic integration with the solar power systems. RO is adequate for peak-shaving allowing for a reduction of electrochemical battery capacity while the MED is capable of benefitting of "free" low temperature heat recoverable by power cycles.

The result is the possibility of fulfilling the electricity and potable water demand of the island community with a very high ($> 80\%$) RES penetration at lower overall cost than the traditional, fossil fuel based, solution.

Reference

[1] IRENA, Renewable Desalination: Technology Options for Islands, (2015).
[2] I.C. Karagiannis, P.G. Soldatos, Water desalination cost literature: review and assessment, Desalination 223 (1–3) (2008) 448–456.
[3] J. Schallenberg-Rodriguez, J.M. Veza, A. Blanco-Marigorta, Energy efficiency and desalination in the Canary Islands, Renew. Sust. Energ. Rev. 40 (2014) 741–748.
[4] IRENA-GREIN, A Path to Prosperity: Renewable Energy for Islands, (2014).
[5] GREIN, Global Renewable Energy Islands Network, [Online]. Available: http://grein.irena.org/UserFiles/Images/GREIN_brochure_EN_WEB_single page.pdf. [Accessed: (26-Aug-2016).
[6] IRENA, Off-Grid Renewable Energy Systems: Status and Methodological Issues, (2015).
[7] K. Bunker, S. Doig, K. Hawley, J. Morris, Renewable Microgrids: Profiles from Islands and Remote Communities Across the Globe (no.), (November, 2015).
[8] C. Bueno, J.A. Carta, Technical–economic analysis of wind-powered pumped hydrostorage systems. Part II: model application to the island of El Hierro, Sol. Energy 78 (3) (Mar. 2005) 396–405.
[9] Q. Ma, H. Lu, Wind energy technologies integrated with desalination systems: review and state-of-the-art, Desalination 277 (1–3) (Aug. 2011) 274–280.
[10] E. Cardona, A. Piacentino, F. Marchese, Performance evaluation of CHP hybrid seawater desalination plants, Desalination 205 (1–3) (2007) 1–14.
[11] G. Iaquaniello, A. Salladini, A. Mari, A.A. Mabrouk, H.E.S. Fath, Concentrating solar power (CSP) system integrated with MED-RO hybrid desalination, Desalination 336 (1) (2014) 121–128.
[12] S. Mazzola, M. Astolfi, E. Macchi, A detailed model for the optimal management of a multigood microgrid, Appl. Energy 154 (Sep. 2015) 862–873.
[13] S. Casimiro, J. Cardoso, C. Ioakimidis, J. Farinha Mendes, C. Mineo, A. Cipollina, MED parallel system powered by concentrating solar power (CSP). Model and case study: Trapani, Sicily, Desalin. Water Treat. (2014) 1–14 (no. March 2015).
[14] H. Pombeiro, A. Pina, C. Silva, Analyzing residential electricity consumption patterns based on consumer's segmentation, CEUR Workshop Proceedings, 2012, pp. 29–38.
[15] A. Funk, W.B. DeOreo, Embedded Energy in Water Studies Study 3: End-use Water Demand Profiles, 1 (2011), p. 215.
[16] IRENA, Water Desalination Using Renewable Energy, (2012).
[17] C.R. Bartels, K. Andes, Consideration of energy savings in SWRO, Desalin. Water Treat. 51 (4–6) (Jan. 2013) 717–725.
[18] V.G. Gude, N. Nirmalakhandan, S. Deng, Renewable and sustainable approaches for desalination, Renew. Sust. Energ. Rev. 14 (9) (2010) 2641–2654.
[19] A. Ophir, F. Lokiec, Advanced MED process for most economical sea water desalination, Desalination 182 (1–3) (2005) 187–198.
[20] E. Macchi, M. Astolfi, Organic Rankine Cycle (ORC) Power Systems, first ed., Woodhead Publishing, 2016.
[21] S. Mazzola, M. Astolfi, E. Macchi, The potential role of solid biomass for rural electrification: a techno economic analysis for a hybrid microgrid in India, Appl. Energy 169 (2016) 370–383.
[22] N. R. E. Laboratory, System Advisor Model Version 2016.3.14 (SAM 2016.3.14), [Online]. Available: https://sam.nrel.gov/content/downloads . [Accessed: (12-Sep-2016).
[23] NREL, Energy Transition Initiative: Playbook, (2015).
[24] S. Drouilhet, B. Johnson, S. Drouilhet, B. Johnson, A battery life prediction method for hybrid power applications, 35th Aerospace Sciences Meeting and Exhibit, 1997.
[25] P. Kurup, C.S. Turchi, Parabolic Trough Collector Cost Update for the System Advisor Model (SAM), (November, 2015).
[26] S. Lemmens, A perspective on costs and cost estimation techniques for organic Rankine cycle systems, 3rd International Seminar on ORC Power Systems, 2015.
[27] F. Banat, Economic and technical assessment of desalination technologies, IWA Conf. Technol. Water…, 2007.
[28] U. Herrmann, B. Kelly, H. Price, Two-tank molten salt storage for parabolic trough solar power plants, Energy 29 (5–6) (Apr. 2004) 883–893.
[29] J.E. Pacheco, S.K. Showalter, W.J. Kolb, Development of a molten-salt thermocline thermal storage system for parabolic trough plants, J. Sol. Energy Eng. 124 (2) (2002) 153.